HHS Public Access

Author manuscript

Cancer Res. Author manuscript; available in PMC 2022 April 15.

Published in final edited form as:

Cancer Res. 2021 October 15; 81(20): 5296–5310. doi:10.1158/0008-5472.CAN-21-0757.

Dietary fats high in linoleic acids impair anti-tumor T cell responses by inducing E-FABP-mediated mitochondrial dysfunction

Rong Jin[1,2], **Jiaqing Hao**[1], **Yanmei Yi**[1,3], **Di Yin**[1,4], **Yuan Hua**[1], **Xiaohong Li**[5], **Hanmei Bao**[6], **Xianlin Han**[6,7], **Nejat K. Egilmez**[1], **Edward R. Sauter**[8], **Bing Li**[1,*]

[1]Department of Microbiology and Immunology, University of Louisville, Louisville, KY, USA.

[2]Department of Immunology, School of Basic Medical Sciences, Peking University, Beijing, China.

[3]Department of Histology and Embryology, Guangdong Medical University, Zhanjiang, China.

[4]School of Basic Medical Sciences, Guangdong Medical University, Guangzhou, China.

[5]Kentucky Biomedical Research Infrastructure Network Bioinformatics Core, Department of Anatomical Sciences and Neurobiology, University of Louisville, Louisville, KY, USA

[6]Barshop Institute for Longevity and Aging Studies, University of Texas Health Science Center at San Antonio, San Antonio, TX

[7]Department of Medicine, University of Texas Health Science Center at San Antonio, San Antonio, TX

[8]Division of Cancer Prevention, NIH/NCI, Bethesda, MD, USA

Abstract

The most recent American Dietary Guidelines (2020-2025) recommend shifting dietary fats from solid saturated fats to unsaturated oils. Dietary oils contain different compositions of unsaturated fatty acids (UFA). Oleic acid (OA) and linoleic acid (LA) are the most common UFA in dietary oils. How individual UFA in oils regulate immune cell function and cancer risk remains unclear. Here we demonstrated that high fat diets (HFD) rich either in OA or LA induced a similar degree of murine obesity, but the LA-rich HFD specifically promoted mammary tumor growth. LA impaired anti-tumor T cell responses by promoting naïve T cell apoptosis and inhibiting TNFα production. While exogenous OA and LA were taken up by T cells with similar efficacy, only LA induced significant mitochondrial ROS production and lipid peroxidation. Importantly, naïve T cells predominantly expressed epidermal fatty acid binding protein (E-FABP), which is central in facilitating LA mitochondrial transport and cardiolipin incorporation. Genetic depletion of E-

*Correspondence to: Bing Li, Associate Professor at the Department of Microbiology and Immunology, University of Louisville. Address: 505 South Hancock Street, Louisville, KY 40202, USA, b.li@louisville.edu.

R. Jin, and J. Hao contributed equally to this article.

Author's contributions

J.R., H.J., Y.Y., Y.D., Y.H., H.B., performed research; J. R. , H.J. and L.B. analyzed data. J.R. and L.X. carried out the microarray analysis. H.X., E.N., S.E. and L.B. contributed to research design and manuscript writing. L.B. supervised the whole project, designed the research and wrote the manuscript. All authors discussed the results and commented on the manuscript.

Disclosure of Potential Conflicts of Interest

The authors state no conflict of interest

FABP rescued LA-impaired T cell responses and suppressed LA-rich HFD-associated mammary tumor growth. Collectively, these data suggest that dietary oils high in LA promote mammary tumors by inducing E-FABP-mediated T cell dysfunction.

Significance—These findings suggest that modulation of dietary oil composition and inhibition of E-FABP activity may represent novel strategies to enhance T cell function in the prevention and treatment of obesity-associated cancers.

Introduction

Fats are essential nutrients in human diets (1). They form cellular components (*e.g.* cell membrane), supply energy and facilitate absorption of fat-soluble nutrients (*e.g.* vitamins D). As the backbone of dietary fats, fatty acids (FA) include saturated FA (SFA), monosaturated FA (MUFA), and polyunsaturated FA (PUFA) depending on the numbers of double bonds in the aliphatic chain. SFA have linear structure while *cis* unsaturated FA exhibit a bent shape due to the double bond. As such, saturated fats rich in linear SFA are tightly packed and therefore are solid (*e.g.* butter) whereas oils rich in bent UFA are loosely packed and are liquid at room temperature (*e.g.* soybean oil). Despite different FA components in various dietary fat sources, consumption of high fat diets (HFD) has generally been linked to the epidemic of obesity (2,3).

Obesity is associated with an increased risk of cardiovascular disease (CVD), type 2 diabetes and many types of cancer (4,5). To improve overall health and prevent obesity-related chronic diseases, the most recent Dietary Guidelines (2020-2025) for Americans recommend a healthy eating pattern with an emphasis of shifting dietary fats from solid saturated fats to unsaturated oils (https://health.gov/our-work/food-nutrition/2015-2020-dietary-guidelines/guidelines/). This recommendation is based on the consistent observations that replacing saturated with unsaturated fats lowers blood levels of low-density lipoprotein (LDL) and reduces the risk of CVD and related death (6). Despite their benefits in CVD prevention, whether dietary oils, which are mainly composed of 18:1 oleic acid (OA) and 18:2 linoleic acid (LA), reduce the risk of other obesity-associated diseases (*e.g.* cancer development) needs to be elucidated. Moreover, how individual unsaturated FA in dietary oils regulate immune cell metabolism and functional outcome remains largely unknown.

It is now well established that the immune system, particularly T cells, can play a critical role in controlling cancer development and progression. Mounting evidence has demonstrated that FA metabolism has profound effects on the differentiation, function and survival of T cells (7). Naïve T cells are known to exhibit a quiescent metabolic state, and T cell activation requires both aerobic glycolysis and *de novo* lipid synthesis for their proliferation and function (8,9). Unlike activated effector T cells, naïve and regulatory T cells (Tregs) rely more on FA oxidation and less on glycolysis for their appropriate differentiation (10). Of note, obesity raises circulating levels of free FA, which can induce T cell death through a process known as lipotoxicity (11). Saturated FA appear more lipotoxic than unsaturated FA to T cells and other immune cells (*e.g.* macrophages), but Tregs seem more tolerant to saturated FA due to their enhanced FA uptake and oxidation pathways (11,12). Thus, it is pivotal to understand the cellular and molecular mechanisms by which

individual FA regulate phenotypic and functional output in different T cell subsets in the setting of obesity and cancer.

Due to the low solubility of long-chain dietary FA, a family of FA binding proteins (FABPs) has been evolved to facilitate FA trafficking and responses inside different cells (13,14). Among the 9 members of the FABP family, E-FABP (also known as FABP5) is highly expressed in T cells and promotes Th17 cell differentiation in an experimental autoimmune encephalomyelitis model (15,16). Recent studies demonstrated that E-FABP facilitates the uptake of exogenous FA and promotes the survival of tissue-resident memory T cells (17). Inhibition of E-FABP function in regulatory T cells impairs their lipid metabolism, but enhances their suppressive activity (18). Despite the emerging evidence showing a pivotal role for E-FABP in regulating lipid metabolism and the functional properties of different T cell subsets, it is mechanistically unclear how it regulates individual FA metabolism and determines T cell fate.

Given the recently updated US healthy diet guidelines with an emphasis on oils, we conducted studies *in vitro* and in clinically relevant obese mouse models to determine whether and how different FA in dietary oils regulate T cell survival and function. Findings from these studies demonstrated that oils rich in 18:2 LA, but not 18:1 OA, impair T cell survival and anti-tumor function by a novel E-FABP-mediated mechanism involving LA-induced mitochondrial dysfunction in naïve T cells.

Materials and Methods

Mice

E-FABP-deficient mice (E-FABP$^{-/-}$), their wild type (WT) littermates, and MMTV-TGFα transgenic mice (all C57BL/6 background) were bred and housed in the animal facility of the University of Louisville. All animal manipulations were carried out according to the protocol approved by the Institutional Animal Care and Use Committee at the University of Louisville. Four-week-old weaned female mice were fed one of three custom-made diets: low fat diet (LFD, 10% fat), safflower oil high fat diet (HFD, 45% fat, rich in 18:2 linoleic acid), or olive oil HFD (45% fat, rich in 18:1 oleic acid), for 4 months before they were euthanized for immune cell phenotype analysis or tumor implantation. Mouse body weight was monitored biweekly.

Cell Lines

The murine E0771 Breast cancer cell line was purchased from CH3BioSystems (Sku: 940001). Cells were maintained in 1640 RPMI media supplemented with 10% GIBCO serum,1% Penstrep and 1% L-Glut and 55 mM β-mercaptoethanol, under 5% CO2 atmospheric oxygen, at 37 °C in a humidified incubator. Further authentication of the cell line was performed by VRL and all pathogens (e.g. mycoplasma, and different mouse viruses) monitored were negative. Cells were cultured for two passages before being implanted in the fourth breast pad of HFD- or LFD-fed female mice for 4 months.

Mammary tumor models

For syngeneic tumor models, 5×10^5 E0771 cells derived from a C57BL/6 mouse mammary adenocarcinoma were orthotopically implanted into the fat pad of the 4th mammary gland of lean or obese mice on different diets. Tumor growth was monitored at 3-day intervals with calipers and tumor volume was calculated by the formula 0.4× (large diameter) × (small diameter)^2. Tumors were weighed when mice were euthanized at the IACUC end point. As described in our previous studies (19), starting from 4 weeks old after weaning MMTV-TGFα female mice, which develop mammary tumors slowly over time (20), were fed the LFD, safflower oil or olive oil HFD for 18 months. Primary mammary tumor development was monitored biweekly. Mammary tumors/mammary tissue were collected for hematoxylin and eosin (H&E) staining and histopathology analysis. To measure tumor infiltrating lymphocytes in the tumor stroma, single cells were separated in a digestion buffer including a final concentration of 500 μg/mL collagenase type 2, 20 μg/mL DNase I and 200 μg/mL type V hyaluronidase at 37 °C for 45 mins. Single cells from thymus, bone marrow, peritoneum, blood, lymph nodes and spleen of tumor-bearing mice were also collected for phenotypic and functional analyses.

Primary Cell Culture

Splenocytes from 6-8 weeks old mice that received a normal diet and cultured with RPMI-1640 supplemented 5% FBS were evaluated *in vitro* assays including apoptosis, intracellular cytokine production and ROS/Mitospy/Mitosox detection (see details in the Supplementary Data).

FA preparation

Endotoxin-free BSA (Cat# AK8917, Akron) was prepared in PBS with a 2mM stocking concentration. Different FAs, including OA (Cat# S-1120,Nu-Chek Prep) and LA (Cat# S-1127,Nu-Chek Prep) were sonicated until dissolved at a stocking concentration of 5mM with the BSA as previously described (21,22).

Lipid uptake, content and lipid peroxidation

Lipid uptake was assessed by incubating splenocytes with 1μM C16-BODIPY (Cat# D-3821, Thermo Fisher) in complete RPMI for 30 mins at 37°C + 5% CO2. For analysis of lipid content, Bodipy-493/503(Cat# D-3922, Thermo Fisher) staining was performed in complete media at 37°C + 5% CO2 for 30 mins. Cell surface CD4 and CD8 were stained with fluorescence conjugated antibodies for 30mins on ice for flow analysis.

For the analysis of lipid peroxidation, splenocytes were treated with 400 μM LA, OA or BSA control for 4 hours, cells were washed once with 1 × PBS, fixed and permeabilized with Transcription Factor Staining Buffer Set (Cat# 00-5523-00, Invitrogen) according to the manufacturer's protocol. Cells were stained with anti-4 Hydroxynonenal (HNE) antibody (1:100, ab48506) at 4°C overnight. After washing with permeabilization buffer, cells were stained with APC-conjugated F(ab)2 fragment Goat anti-Rabbit IgG(H+L) (1:500, Cat# 111-136-144, ImmunoResearch) for 30min on ice before the flow cytometric analysis.

Analysis of Metabolic Phenotyping in T cells

Mitochondrial oxygen consumption rate (OCR) and extracellular acidification rate (ECAR) were measured using the Seahorse XFe bioanalyzer. $3x10^5$ purified T cells per well (>3 wells per sample) were spun onto Cell-Tak (Cell and Tissue Adhesive, Cat# C354240, Fisher Scientific) coated seahorse 96 well plates and preincubated in Seahorse XF OCR media (XF Base medium + 2 mM glutamine + 1 mM sodium pyruvate + 10 mM glucose) or ECAR medium (XF Base medium + 2 mM glutamine) at 37°C for a minimum of 45 mins in the absence of CO_2. OCR was measured under basal conditions, and after the addition of the following drugs: 1 μM oligomycin, 1.5 μM flurorcarbonyl cyanide phenylhydrazone (FCCP) and 0.5μM Rotenone plus Antimycin A at the indicated time point. Measurements were taken using an Extracellular Flux Analyzer (Seahorse bioscience). ECAR was measured under basal conditions, and after the addition of the following drugs: 10 mM glucose, 1.5 μM oligomycin and 50 mM 2-DG as indicated. Measurements were taken using an Extracellular Flux Analyzer (Seahorse bioscience).

Cadiolipin quantification analysis

Splenic T cells were purified from 8-week-old E-FABP$^{-/-}$ and WT mice fed a LFD diet. $3x10^6$ /well T cells were treated with 400μM LA, OA or BSA control in RPMI-1640 supplemented with 5% FBS overnight. Cells were collected and washed once with PBS. Lipid species were analyzed using multidimensional mass spectrometry-based shotgun lipidomic analysis (23). In brief, WT and E-FABP$^{-/-}$ T cell pellet homogenate containing approximately 0.065 mg of protein which was determined with a Pierce BCA assay was accurately transferred to a disposable glass culture test tube. A premixture of lipid internal standards (IS) was added prior to conducting lipid extraction for quantification of the targeted lipid species. Lipid extraction was performed using a modified Bligh and Dyer procedure (24), and each lipid extract was reconstituted in chloroform : methanol (1:1, v:v) at a volume of 1500 μL/mg protein. For shotgun lipidomics, the lipid extract was diluted to a final concentration of ~500 fmol total lipids per μL. Mass spectrometric analysis was performed on a Q Exactive mass spectrometer (Thermo Scientific, San Jose, CA), equipped with an automated nanospray device (TriVersa NanoMate, Advion Bioscience Ltd., Ithaca, NY). Identification and quantification of cardiolipin and cardiolipin species were performed using an automated software program. Result were normalized to the protein content (nmol lipid/mg protein).

Other common methods, including flow cytometry, confocal analysis, real-time PCR and PCR primer sequences (Table S1), ELISA and multiplex cytokine and metabolic panel analyses are shown in the Supplementary data.

Statistical analysis

Flow cytometry data were analyzed using FlowJo 10 (BD Biosciences). Metabolic data were collected with Wave Software Version 2.4 (Agilent). Confocal data were analyzed with FV10-ASW Viewer software (Ver 3.1). Statistical Analysis was performed using Prism 8 software (GraphPad) and results are represented as Mean ± SEM, unless otherwise indicated. Comparisons for two groups were calculated using unpaired two-tailed Student's *t* tests. A p value of <0.05 is regarded as statistically significant.

Results

Olive or safflower oil diet induces a similar degree of murine obesity

It is generally believed that oils rich in MUFA and PUFA are healthier than solid fats high in SFA and *trans*-fat. Common dietary oils are mainly composed of 18:1 OA and 18:2 LA (Table S2). Olive oil mainly contains OA (71.3%) and safflower oil is high in LA (75.7%) (Figure 1A), we selected these two oils in our studies as they represent high content OA or LA. A typical American diet is usually high in fat intake (35% fat) (25). We designed custom HFDs containing either 35% olive oil or 35% safflower oil, respectively. Our control low fat diet (LFD) contained neither olive nor safflower oil. To avoid confounding effects that normally exist in human diets, our custom murine diets were identical in ingredients except for the fat content (Figure 1B). Weaned female mice (3-4 weeks old) were randomly grouped and fed the safflower oil, olive oil or control LFD, respectively. Both HFDs significantly increased murine body weight compared to the LFD ($p<0.001$), but weight gain was similar between the safflower and olive oil groups (Figure 1C). We also analyzed fat deposition in these mice (Figure 1D). There was a similar increase in fat deposition after the consumption of either safflower or olive oil HFD (Figure 1E). Common metabolic parameters, including leptin, adiponectin, resistin, insulin and MCP-1 were also similar between safflower oil and olive oil-fed mice (Figure 1F-1J). These results demonstrated that, regardless of the different FA compositions, safflower and olive oil diets induced a similar degree of obesity in mouse models.

Mice fed the safflower oil diet exhibit impaired T cell responses

Obesity negatively affects multiple aspects of immune activity (26). To evaluate whether obesity induced by consumption of the olive or safflower oil impacts the immune system, and to what degree, we first analyzed the immune cell phenotype in major immune tissues/organs, including bone marrow (BM), thymus, spleen, lymph nodes (LN), blood, and peritoneum (PT). Phenotypically, as compared to the LFD, neither the olive nor safflower oil diet had a major impact on DCs, macrophages, B cells and NK cells in different immune organs/tissues (Figure S1A-S1D). However, the percentage of T cells, particularly $CD8^+$ T cells, were remarkably reduced in the peripheral blood (Figure 2A, 2B) and in the spleen (Figure 2C, 2D) of mice fed the safflower compared to the olive oil diet or LFD. The total numbers of $CD8^+$ and $CD4^+$ T cells were also significantly decreased in mice fed the safflower oil diet (Figure 2E, 2F). The safflower oil diet neither influenced the development nor reduced the number of T cells in the thymus (Figure S1E, S1F), suggesting that the negative impact of safflower oil on T cells occurs in the peripheral, but not in the central organ where T cells differentiate. Given the phenotypic alterations in T cells, we next measured serum levels of T cell-derived cytokines in these mice. Consumption of safflower or olive oil diet did not affect the serum levels of IL-17 (Figure 2G), IFNγ (Figure 2H), IL-2, IL-4 and IL-10 (Figure S1G-S1I), but significantly reduced TNFα levels (Figure 2I). Intracellular staining demonstrated that TNFα expression in both $CD8^+$ and $CD4^+$ T cells from the safflower oil-fed mice was significantly decreased in the spleen (Figure 2J-2L) and in LNs (Figure S1J-S1K) compared to those from olive oil or LFD-fed mice, while $Foxp3^+$ regulatory T cells were comparable among the groups (Figure S1L). Altogether, these results

indicated that consumption of the safflower oil, but not olive oil diet, selectively reduced T cell prevalence and TNFα production.

Safflower oil diet-fed mice exhibit increased mammary tumor growth and development

Given the impaired T cell prevalence and activity induced by the safflower oil diet, we speculated that tumor immune-evasion in those mice might be enhanced. Using a syngeneic mammary tumor model involving orthotropic implantation of E0771 tumor cells into the mammary fat pad in mice fed the LFD, safflower or olive oil HFD, respectively, we observed a significant acceleration of mammary tumor growth in the safflower oil-fed mice compared to the olive oil or LFD-fed mice (Figure 3A). Tumor weight in mice fed the safflower oil diet was also significantly larger than other groups, even though mice on the olive oil diet were just as obese (Figure 3B, Figure S2A). This observation of uncoupling obesity from tumor growth in mice on the olive oil diet suggests that not all dietary oil-induced obesity is tumorigenic. Our prior studies showed that MMTV-TGFα transgenic mice developed primary mammary tumors (19). Using this MMTV-TGFα transgenic mouse model, we observed that MMTV mice fed the safflower oil diet exhibited an increased incidence and growth of mammary tumors compared to mice fed the olive oil diet or LFD (Figure 3C-3E), further confirming that consumption of the safflower oil diet is associated with an increased risk of mammary tumor development.

As naïve mice fed our safflower oil diet exhibited reduced T cell numbers and impaired T cell function (Figure 2), we next assessed T cell responses in the mammary tumor-bearing mice. Interestingly, tumors from safflower oil-fed mice had reduced infiltration of $CD8^+$ and $CD4^+$ T cells compared to those from LFD or olive oil-fed mice (Figure 3F-3H). The reduction of tumor-infiltrating T cells in the safflower oil-fed mice was further confirmed by both immunohistochemistry and confocal staining (Figure 3I, 3J). We also analyzed T cells in non-tumor tissues and observed reduced $CD8^+$ T cell prevalence in the spleen of safflower oil-fed mice (Figure S2B, S2C). Moreover, we evaluated T cell cytokine production in these tumor-bearing mice and observed that $CD4^+$ and $CD8^+$ T cells in tumors of safflower oil-fed mice exhibited reduced production of TNFα (Figure 3K, 3L), but not IFNγ (Figure 3M, 3N), compared to LFD or olive oil-fed mice. Consistent with these observations, T cells in non-tumor immune organs (*e.g.* spleen) of safflower oil-fed mice showed the same pattern of impaired TNFα production (Figure S2E-S2H), suggesting an important role of TNFα in T cell-meditated anti-tumor activity. Indeed, when we incubated E0771 tumor cells with T cell-produced cytokines, we found that TNFα, but not IFNγ or IL-17, directly induced E0771 tumor cell death (Figure 3O). Collectively, these results suggested that consumption of the safflower oil diet impaired effective anti-tumor T cell responses, leading to enhanced mammary tumor cell evasion and growth.

LA rich in safflower oil impairs T cell responses

To determine the molecular mechanisms by which consumption of the safflower oil diet reduced T cell numbers and TNFα production in mice, we hypothesized that LA in safflower oil was responsible for the impaired T cell responses *in vivo*. To this end, we treated T cells *in vitro* with different concentrations of LA or OA observed under physiological/pathological conditions. In line with *in vivo* data collected from safflower

or olive oil fed-mice, LA, but not OA induced significant death of $CD8^+$ and $CD4^+$ T cells (Figure 4A, 4B). Intracellular staining showed that LA treatment *in vitro* significantly inhibited the production of TNFα (Figure 4C, 4D), but not IFNγ (Figure S3A, S3B), in $CD8^+$ and $CD4^+$ T cells. Quantitative PCR confirmed these results (Figure S3C, S3D). IFNγ was predominantly produced by $CD44^+$ activated T cells whereas TNFα was generated by both $CD44^-$ naïve T cells and $CD44^+$ activated T cells (Figure S3E, S3F). These results suggest that LA mainly affect naïve T cells. Indeed, when T cell death was further analyzed by gating on $CD44^-$ naïve and $CD44^+$ activated T cells, we demonstrated that LA-induced T cell death was significant in naïve, but not activated T cells (Figure S3G, S3H). Consistent with these observations, $CD44^-$ naïve $CD4^+$ and $CD8^+$ T cells were significantly decreased in the safflower oil-fed mice (Figure S3I, S3J). Altogether, our data indicate that LA in safflower oil-fed mice and in culture negatively affect naïve T cell survival and TNFα production.

Lipids are involved in multiple forms of regulated cell death, including apoptosis, necroptosis, and ferroptosis (27). To identify the specific T cell death pathway induced by LA, we included specific inhibitors, including pan-caspase inhibitor z-VAD for apoptosis, necrostatin 1 for necroptosis, and ferrostatin 1 for ferroptosis, in culture media. The data revealed that, z-VAD, but not necrostatin 1 or ferrostatin 1, inhibited LA-induced T cell death (Figure 4E, 4F), suggesting that apoptosis was the main cell death pathway induced by LA treatment. To further dissect how LA-induced apoptosis in T cells, we found that LA treatment dramatically induced the production of reactive oxygen species (ROS) in T cells, which was visualized using confocal microscopy (Figure 4G) and flow cytometric staining (Figure 4H, 4I) by oxidization of DCFDA (2',7'-dichlorofluorescin diacetate) to fluorescent DCF (2',7'- dichlorofluorescein). Moreover, inhibition of ROS with N-acetyl-l-cysteine (NAC), a commonly used ROS scavenger, completely blocked LA-induced T cell death, supporting a pivotal role of ROS in mediating LA-induced T cell apoptosis (Figure 4J, 4K). Of note, neither LA nor OA treatment affected the expression of NADPH oxidases (*e.g.* NOX2, or DUOX1, DUOX2) in T cells (Figure S3K-S3M), and inhibition of NADPH oxidase activity by diphenyleneiodonium chloride (DPI), a specific inhibitor of NADPH oxidases, did not rescue LA-induced T cell death (Figure 4J, 4K). These results imply that LA-induced ROS leading to T cell apoptosis was not generated by the NADPH oxidase-mediated pathway.

LA impairs T cell responses by promoting mitochondrial dysregulation

We next wanted to determine how LA induced non-NADPH-mediated ROS production in T cells. T cells treated with either LA or OA had similar lipid contents (Figure S4A), suggesting no differences in LA and OA uptake by T cells. Furthermore, T cells treated with LA or OA exhibited comparable increase of oxygen consumption in mitochondria (Figure S4B), suggesting similar FA oxidation (FAO) induced by either LA or OA in mitochondria. Interestingly, when we measured the production of mitochondrial ROS (Mitosox) in T cells treated with LA, OA or BSA, we found that LA treatment significantly promoted mitochondrial ROS production in both $CD8^+$ T and $CD4^+$ cells compared to BSA or OA-treated groups (Figure 5A-5C). In line with increased mitochondrial ROS production, LA treatment increased mitochondria, but did not affect peroxisomes in T cells (Figure

5D). In contrast, OA treatment did not induce significant increase of mitochondria in $CD8^+$ and $CD4^+$ T cells (Figure 5E, 5F). Given that 18:2 LA was the predominant composition of cardiolipin (CL), a unique class of phospholipids in mitochondrial inner membrane, and 18:2 LA was more sensitive to ROS-mediated lipid peroxidation than 18:1 OA (28,29), we postulated that treatment with LA, but not OA, would induce mitochondrial lipid peroxidation. Indeed, 4-HNE (4-hydroxynonenal), a common byproduct of lipid peroxidation, was significantly upregulated in both $CD8^+$ and $CD4^+$ T cells in response to LA treatment (Figure 5G-5I). These data demonstrated that LA specifically induced mitochondrial ROS and lipid peroxidation, thus leading to mitochondrial dysfunction in T cells.

When we analyzed a publicly accessible microarray dataset consisting of T cells treated with or without LA (GSE67918) (30), this independent dataset also demonstrated that LA treatment induced oxidative phosphorylation and mitochondrial dysfunction by Ingenuity Pathway Analysis (IPA) (Figure S4C, S4D). Moreover, gene network pathway analysis showed that Cpt1 (carnitine palmitoyltransferase 1), a rate-limiting mitochondrial enzyme catalyzing the transfer of FA from the cytosol to mitochondria, was upregulated in LA-treated T cells (Figure S4E). We also demonstrated that LA and OA treatment induced Cpt1 expression (Figure 5J, Figure S4F, S4G), while other FA-metabolism related molecules, such as acyl-CoA synthase (ACSL), peroxisome proliferator-activated receptor (Ppar) β, PPARγ coactivator (Pgc) 1α, cardiolipin synthase 1 (Crsl1) (Figure S4H-S4K) were not altered by FA treatment, suggesting a specific FA/Cpt1 pathway for mitochondrial FAO. Importantly, when we inhibited Cpt1 activity with etomoxir (Eto), LA-induced mitochondrial ROS production (Figure 5K, 5L) and T cell death (Figure 5M, 5N) were successfully inhibited. Taken together, our data demonstrated that LA induced T cell mitochondrial dysfunction through the Cpt1/mitoROS/lipid peroxidation pathway.

E-FABP is critical in facilitating LA-induced mitochondrial dysregulation

LA and OA are long chain fatty acids (LCFA) which are insoluble in aqueous cytoplasm, and FABPs have been shown to play a central role in coordinating LCFA trafficking and responses inside cells (13,14). To further investigate if FABPs are critical in LA-induced effects in T cells, we first examined the expression profile of FABPs in T cells. Among FABP family members, E-FABP was the predominant form expressed in both $CD8^+$ (Figure 6A) and $CD4^+$ T cells (Figure S5A). We next used T cells from WT or E-FABP-deficient mice to determine the role of E-FABP in T cells (Figure 6B). Although we did not notice obvious differences in endogenous lipid contents between WT and E-$FABP^{-/-}$ T cells (Figure S5B-5C), E-FABP deficiency significantly impaired exogenous FA uptake in $CD8^+$ and $CD4^+$ T cells (Figure 6C). We further compared genes related to FA mitochondrial metabolism between WT and E-$FABP^{-/-}$ T cells. While E-FABP deficiency did not affect the expression of Acsl, Crsl1, Pparβ, cyclooxygenase 2 (Cox2), dynamin-related protein 1 (Drp 1), dominant optic atrophy 1 (Opa 1) (Figure S5D-S5I), Cpt1b and uncoupling protein 2 (Ucp2) expression were dramatically reduced in E-$FABP^{-/-}$ T cells in response to LA treatment (Figure 6D, 6E). In line with these results, LA-induced mitochondrial oxygen consumption (OCR) (Figure 6F) and mitochondrial ROS production (Figure 6G) were significantly decreased in E-$FABP^{-/-}$ T cells compared to WT T cells. These results

demonstrated that E-FABP deficiency alleviated exogenous LA uptake, mitochondrial lipid transport and fatty acid oxidation.

Given the unique and essential roles of cardiolipins (CL) in mitochondrial dynamics and function (31), we next determined if LA-induced mitochondrial dysfunction in T cells was mediated by E-FABP-dependent CL peroxidation. In T cells treated with LA, E-FABP deficiency reduced total CL levels and individual CL species (Figure 6H, 6I). As 18:2 LA was the predominant fatty acyl species in CL (32), we found that 18:2 LA constituted about 78% of the acyl species of CL in T cells from WT and E-FABP deficient mice (Figure S5J). Whereas E-FABP deficiency did not significantly affect CL composition, it reduced individual fatty acyl contents of CL fractions isolated from LA-treated T cells (Figure 6J). Importantly, E-FABP deficiency significantly reduced mitochondrial lipid peroxidation in T cells (Figure 6K). Accordingly, LA-induced T cell death in WT T cells was significantly reduced when E-FABP was absent (Figure 6L). Production of TNFα (Figure 6M, 6N), but not IFNγ (Figure S5K), was also rescued in E-FABP$^{-/-}$ T cells. These data indicated that E-FABP was critical in coordinating LA-induced mitochondrial lipid dysregulation, leading to cell death and impaired T cell functions.

Deficiency of E-FABP attenuates safflower oil-induced tumor growth

Given the essential role of E-FABP in LA-induced effects on T cells *in vitro*, we reasoned that E-FABP deficiency would rescue safflower oil-impaired T cell function and enhance tumor killing *in vivo*. To this end, we fed WT and E-FABP$^{-/-}$ mice the safflower oil diet, and compared T cell responses in these mice. Interestingly, E-FABP deficiency did not affect safflower oil-induced murine obesity (Figure S6A), but significantly reduced ROS production in both CD8^{+} and CD4^{+} T cells (Figure S6B, S6C). Accordingly, more CD8^{+} and CD4^{+} T cells survived in E-FABP$^{-/-}$ mice compared to WT mice (Figure S6D, S6E). When we measured T cell cytokine production, we also observed that CD8^{+} and CD4^{+} T cells in E-FABP$^{-/-}$ mice produced more cytokines, particularly TNFα, than those in WT mice (Figure S6F-S6I). Our *in vivo* data from diet-induced obese mice suggested that E-FABP deficiency improved safflower oil HFD-impaired T cell survival and function.

To determine if the impaired anti-tumor T cell function induced by the safflower oil diet (Figure 3) can be rescued by E-FABP deficiency, we orthotopically implanted E0771 mammary tumor cells in safflower oil-induced obese WT and E-FABP$^{-/-}$ mice. Although E-FABP$^{-/-}$ and WT mice had a similar degree of obesity (Figure S6J), tumor growth was significantly inhibited in E-FABP$^{-/-}$ mice (Figure 7A). Accordingly, tumor weight in E-FABP$^{-/-}$ mice was 50% of tumors in WT mice (Figure 7B). Both immunohistochemistry and confocal staining demonstrated more CD8^{+} T cell infiltration in the tumor stroma of E-FABP$^{-/-}$ mice (Figure 7C, 7D). Flow cytometric staining confirmed more tumor infiltrating CD8^{+} and CD4^{+} T cells in E-FABP$^{-/-}$ mice than WT mice (Figure 7E, 7F). In line with non-tumor-bearing obese mice, splenic CD8^{+} and CD4^{+} T cells in tumor-bearing mice were also higher (Figure 7G, 7H) with reduced levels of ROS production (Figure 7I, 7J) when E-FABP was genetically depleted. Moreover, we measured T cell cytokine production in tumor-bearing mice. E-FABP$^{-/-}$ T cells exhibited increased TNFα production both in tumor stroma and in the spleen (Figure 7K-7N), but IFNγ levels were comparable in WT

and E-FABP$^{-/-}$ mice (Figure S6K-S6N). When we compared serum levels of cytokines and FABPs in WT and E-FABP$^{-/-}$ mice, only E-FABP levels were significantly different (Figure S6O-S6S), suggesting a T cell-mediated local anti-tumor response. As E-FABP was also expressed in other cells (33), to further verify the specific role of E-FABP in regulating T cell anti-tumor function, we adoptively transferred WT and E-FABP$^{-/-}$ CD8^{+} T cells to tumor-bearing safflower oil-fed WT mice. Tumor growth in WT→WT mice was significantly faster than tumors in E-FABP$^{-/-}$→WT mice (Figure 7O). Tumor size and weight in WT→WT group were significantly larger than E-FABP$^{-/-}$→WT group (Figure 7P, 7Q). There were also increased tumor-infiltrating CD8^{+} T cells in E-FABP$^{-/-}$→WT mice (Figure 7R). These results clearly demonstrated that E-FABP expression in CD8^{+} T cells was critical in mediating safflower oil-impaired T cell responses.

Discussion

A healthy diet is essential to the maintenance and improvement of overall health. As essential nutrients in healthy diets, dietary fats are generally composed of saturated solid fats and unsaturated oils. The 2020-2025 Dietary Guidelines for Americans recommends replacing solid fats with oils due to mounting evidence showing that oils protect from the development and mortality of CVD. However, depending on the fat source, oils can have different unsaturated FA composition (*e.g.* MUFA and PUFA). It is of great interest to determine which oils are healthier than others and how individual unsaturated FA in different oils exert their biological effects *in vivo*.

OA and LA are the two main unsaturated FA in dietary oils. To assess the biological functions of OA and LA, we fed mice with custom-made olive oil and safflower oil HFDs which are rich in OA and LA, respectively. Epidemiologic evidence suggests that olive oil, an important component of the Mediterranean diet, is a healthy oil whereas safflower oil does not have similar evidence supporting its health benefits (34,35). Due to many confounding factors in human diets, clinical trials evaluating the effect of specific FA (*e.g.* LA) in the risk of breast cancer have not reached conclusive results (36,37). The mechanism(s) driving this perceived benefit of olive but not safflower oil is unclear. Unlike short (< 7 carbon) and medium (7-13 carbon) chain FA which can directly enter the capillaries and are carried to liver for process through the portal vein (38), long chain FA (>13 carbon) in diets enter the lymphatic and then blood circulation through lacteals without liver processing. Thus, long chain FA in dietary fats may exert a direct lipotoxic effect on circulatory immune cells. Indeed, when we analyzed immune cell phenotypes in mice fed different dietary oils, we noticed that T cells, but not other major immune cells (*e.g.* lipid-laden monocytes/macrophages), in the blood and spleen were significantly reduced in safflower oil-fed but not olive oil or LFD-fed mice, suggesting that LA high in safflower oil exerts a specific role in T cells. Of note, levels of free non-esterified FA in the circulation usually range from 200-400μM in healthy individuals and 400-800μM in obese and/or diabetic patients (39). Using these physiological/pathological levels of LA or OA to treat T cells *in vitro*, we demonstrated that LA, but not OA, induced a dose-dependent T cell death, which mirrored the *in vivo* observations of reduced T cells in safflower oil-fed mice. In combination with our previous studies demonstrating that similar levels of saturated

FA, but not unsaturated FA, induced macrophage cell death (12), our findings suggest that individual FA exhibit unique effect on different immune cell subsets.

Besides inducing T cell death, consumption of the safflower oil diet also impaired T cell responses. Specifically, T cells from safflower oil-fed mice exhibited reduced levels of TNFα, but not IFNγ, compared to these from olive oil or LFD-fed mice. Consistently, treatment of T cells with LA *in vitro* inhibited the production of TNFα. Interestingly, TNFα can be produced by both naïve and activated T cell subsets whereas IFNγ is only produced by activated T cells (40,41). Given the unaltered IFNγ but reduced TNFα responses in T cells observed *in vitro* and *in vivo*, our data demonstrate that LA in safflower oil preferentially induces naïve T cell death and impairs their function. Indeed, metabolic profiling has demonstrated that FAO is the primary energy source for naïve T cells whereas activator T cells mainly rely on aerobic glycolysis to meet their metabolic demands (42,43). Compared to unstimulated naïve T cells, activated T cells exhibited dramatically reduced FA oxidation (44). These studies support our observations that naïve T cells are more sensitive to exogenous LA than activated T cells.

We further determined the molecular mechanisms by which LA specifically induced T cell death and found that LA-induced T cell death was rescued either by pan-caspase inhibitors (*e.g.* z-VAD) or by ROS inhibition with NAC, indicating that LA-mediated ROS signaling was responsible for the induction of T cell apoptosis. Although OA and LA were taken up by T cells with similar efficiency, only LA induced significant production of mitochondrial ROS in T cells. Furthermore, inhibition of the mitochondrial FA transport enzyme Cpt1 by etomoxir suppressed LA-induced mitochondrial ROS production and T cell death, confirming that mitochondrial ROS is essential to the LA-mediated effect. As the most common oxidants, ROS include hydrogen peroxide, lipid peroxides (ROOH), superoxide, peroxyl, and hydroxyl (45). Mounting evidence suggests that ROS-induced lipid peroxidation plays a critical role in multiple forms of cell death (46). Further investigation into how LA, but not OA, induced ROS-mediated T cell death revealed that: 1) PUFA (*e.g.* LA) are preferentially oxidized by lipid oxidation; 2) cardiolipins (CL) are a unique class of phospholipids essential for mitochondrial membrane structure and function; 3) 18:2 LA is the dominant acyl group in CL; 4) dietary PUFA have been shown to incorporate into the tetra-acyl pool of CL (28,47,48). These findings collectively suggest that dietary LA induces T cell death through CL incorporation and ROS-mediated lipid oxidation. Indeed, we demonstrate that LA treatment enhances production of mitochondrial ROS and 4-HNE, a specific lipid peroxidation product (49). Thus, our data suggest a novel mechanism by which dietary LA, but not OA, induces T cell apoptosis through mitochondrial ROS-mediated mitochondrial membrane lipid peroxidation, leading to mitochondrial dysfunction and impaired T cell responses.

T cell dysfunction is associated with tumor evasion (50). Using murine mammary tumor models, we demonstrated that increased tumor growth in safflower oil-fed mice was associated with reduced T cell infiltration and TNFα production in the tumor stroma. Of note, mammary tumor cells (e.g. E0771 cells) did not exhibit obvious alterations in survival and proliferation in response to LA treatment, suggesting that impaired T cell immunity is mainly responsible for the increased mammary tumor growth in the

safflower oil-fed mice. To further delineate how insoluble dietary LA was able to induce T cell dysfunction, we demonstrated that E-FABP expressed in T cells was critical in chaperoning LA-trafficking, mitochondrial ROS production, and lipid peroxidation. First, as the predominant FABP member in naïve T cells, E-FABP facilitates uptake of exogenous FA. Second, E-FABP coordinates with Cpt1 for mitochondrial transport as E-FABP deficiency reduces Cpt1 expression in T cells. Third, E-FABP expression promotes FA-mediated FAO in mitochondria as evidenced by elevated oxygen consumption in E-FABP-sufficient T cells. Fourth, E-FABP promotes LA incorporation into different species of CL in the mitochondrial membrane, leading to elevated lipid peroxidation and T cell apoptosis. Finally, safflower oil diet-induced mammary tumor growth in mice was mitigated when E-FABP was genetically depleted. E-FABP is also expressed other cells (*e.g.* macrophages), and our previous study showed that E-FABP expression in macrophages enhanced anti-tumor responses in non-obese models (33). To evaluate the specific role of E-FABP in mediating safflower oil-impaired T cell responses, adoptive transfer of $CD8^+$ T cells from safflower oil-fed E-$FABP^{-/-}$, but not WT mice, was shown to inhibit mammary tumor growth, confirming a specific role of E-FABP in mediating safflower oil-impaired anti-tumor function of CD8+ T cells in obese mice. Thus, our studies suggest that E-FABP, as an essential FA sensor in immune cells, facilitates normal FA metabolism for anti-tumor responses in non-obese conditions, but impairs tumor immunosurveillance by enhancing dysregulated mitochondrial lipid peroxidation in the safflower oil HFD-induced obese setting. Of note, while E-FABP can chaperone different dietary FA, including LA and OA, but only LA, but not OA, can induce mitochondrial dysfunction, indicating that other factors, including FA structure, more double bonds in LA than OA, which are subject to lipid peroxidation, and enrichment of LA in the mitochondrial inner membrane, also determine cellular functions.

In summary, our studies demonstrated several novel concepts. While obesity could be induced by consumption of either safflower or olive oil HFDs, the immune status underlying the seemingly same degree of obesity was dramatically different. In contrast to OA-rich olive oil, LA-rich safflower oil impaired naïve T cell responses by inducing mitochondrial ROS-mediated lipid peroxidation and dysfunction, which corresponds to impaired T cell responses and increased tumor evasion. Importantly, we identified that E-FABP expression in T cells played a critical role in coordinating LA-mediated FAO and mitochondrial lipid peroxidation. Depletion of E-FABP inhibited safflower oil-exacerbated tumor growth. Thus, our results suggest that while American Dietary Guidelines encourage consumption of liquid (oils) over solid fats as part of a healthy diet, oils high in LA may impair T cell responses and increase tumor risk. Moreover, inhibiting E-FABP activity may represent a novel strategy for T cell-mediated immunotherapy in obesity-associated diseases.

Supplementary Material

Refer to Web version on PubMed Central for supplementary material.

Acknowledgement

We thank the funding support from NIH grants R01CA180986 and R01AI137324. We thank Dr. Steven P. Mathis from the Functional Microbiomics Core at the University of Louisville for analysis of Millipore multiplex

adipokine and cytokine panels. Measurement of cardiolipin in T cells was partially supported by the Mass Spectrometry Core Facility at the Barshop Institute for Longevity and Aging Studies, University of Texas Health Science Center at San Antonio. The opinions expressed in this paper are the authors' own and do not reflect the view of the National Institutes of Health, the Department of Health and Human Services, or the United States government.

References

1. Liu AG, Ford NA, Hu FB, Zelman KM, Mozaffarian D, Kris-Etherton PM. A healthy approach to dietary fats: understanding the science and taking action to reduce consumer confusion. Nutr J 2017;16(1):53 doi 10.1186/s12937-017-0271-4. [PubMed: 28854932]
2. Hu S, Wang L, Yang D, Li L, Togo J, Wu Y, et al. Dietary Fat, but Not Protein or Carbohydrate, Regulates Energy Intake and Causes Adiposity in Mice. Cell Metab 2018;28(3):415–31 e4 doi 10.1016/j.cmet.2018.06.010. [PubMed: 30017356]
3. Buckley J. Availability of high-fat foods might drive the obesity epidemic. Nat Rev Endocrinol 2018;14(10):574–5 doi 10.1038/s41574-018-0084-3. [PubMed: 30158548]
4. Khandekar MJ, Cohen P, Spiegelman BM. Molecular mechanisms of cancer development in obesity. Nat Rev Cancer 2011;11(12):886–95 doi 10.1038/nrc3174. [PubMed: 22113164]
5. Hopkins BD, Goncalves MD, Cantley LC. Obesity and Cancer Mechanisms: Cancer Metabolism. J Clin Oncol 2016;34(35):4277–83 doi 10.1200/JCO.2016.67.9712. [PubMed: 27903152]
6. Sacks FM, Lichtenstein AH, Wu JHY, Appel LJ, Creager MA, Kris-Etherton PM, et al. Dietary Fats and Cardiovascular Disease: A Presidential Advisory From the American Heart Association. Circulation 2017;136(3):e1–e23 doi 10.1161/CIR.0000000000000510. [PubMed: 28620111]
7. Howie D, Ten Bokum A, Necula AS, Cobbold SP, Waldmann H. The Role of Lipid Metabolism in T Lymphocyte Differentiation and Survival. Front Immunol 2017;8:1949 doi 10.3389/fimmu.2017.01949. [PubMed: 29375572]
8. Lee J, Walsh MC, Hoehn KL, James DE, Wherry EJ, Choi Y. Regulator of fatty acid metabolism, acetyl coenzyme a carboxylase 1, controls T cell immunity. J Immunol 2014;192(7):3190–9 doi 10.4049/jimmunol.1302985. [PubMed: 24567531]
9. Resh MD. Covalent lipid modifications of proteins. Curr Biol 2013;23(10):R431–5 doi 10.1016/j.cub.2013.04.024. [PubMed: 23701681]
10. Almeida L, Lochner M, Berod L, Sparwasser T. Metabolic pathways in T cell activation and lineage differentiation. Semin Immunol 2016;28(5):514–24 doi 10.1016/j.smim.2016.10.009. [PubMed: 27825556]
11. de Jong AJ, Kloppenburg M, Toes RE, Ioan-Facsinay A. Fatty acids, lipid mediators, and T-cell function. Front Immunol 2014;5:483 doi 10.3389/fimmu.2014.00483. [PubMed: 25352844]
12. Zhang Y, Rao E, Zeng J, Hao J, Sun Y, Liu S, et al. Adipose Fatty Acid Binding Protein Promotes Saturated Fatty Acid-Induced Macrophage Cell Death through Enhancing Ceramide Production. J Immunol 2017;198(2):798–807 doi 10.4049/jimmunol.1601403. [PubMed: 27920274]
13. Furuhashi M, Hotamisligil GS. Fatty acid-binding proteins: role in metabolic diseases and potential as drug targets. Nat Rev Drug Discov 2008;7(6):489–503 doi 10.1038/nrd2589. [PubMed: 18511927]
14. Li B, Hao J, Zeng J, Sauter ER. SnapShot: FABP Functions. Cell 2020;182(4):1066–e1 doi 10.1016/j.cell.2020.07.027. [PubMed: 32822569]
15. Li B, Reynolds JM, Stout RD, Bernlohr DA, Suttles J. Regulation of Th17 differentiation by epidermal fatty acid-binding protein. J Immunol 2009;182(12):7625–33 doi 10.4049/jimmunol.0804192. [PubMed: 19494286]
16. Rolph MS, Young TR, Shum BO, Gorgun CZ, Schmitz-Peiffer C, Ramshaw IA, et al. Regulation of dendritic cell function and T cell priming by the fatty acid-binding protein AP2. J Immunol 2006;177(11):7794–801 doi 10.4049/jimmunol.177.11.7794. [PubMed: 17114450]
17. Pan Y, Tian T, Park CO, Lofftus SY, Mei S, Liu X, et al. Survival of tissue-resident memory T cells requires exogenous lipid uptake and metabolism. Nature 2017;543(7644):252–6 doi 10.1038/nature21379. [PubMed: 28219080]
18. Field CS, Baixauli F, Kyle RL, Puleston DJ, Cameron AM, Sanin DE, et al. Mitochondrial Integrity Regulated by Lipid Metabolism Is a Cell-Intrinsic Checkpoint for Treg Suppressive

Function. Cell Metab 2020;31(2):422–37 e5 doi 10.1016/j.cmet.2019.11.021. [PubMed: 31883840]

19. Hao J, Zhang Y, Yan X, Yan F, Sun Y, Zeng J, et al. Circulating Adipose Fatty Acid Binding Protein Is a New Link Underlying Obesity-Associated Breast/Mammary Tumor Development. Cell Metab 2018;28(5):689–705 e5 doi 10.1016/j.cmet.2018.07.006. [PubMed: 30100196]
20. Dogan S, Hu X, Zhang Y, Maihle NJ, Grande JP, Cleary MP. Effects of high-fat diet and/or body weight on mammary tumor leptin and apoptosis signaling pathways in MMTV-TGF-alpha mice. Breast Cancer Res 2007;9(6):R91 doi 10.1186/bcr1840. [PubMed: 18162139]
21. Liu L, Jin R, Hao J, Zeng J, Yin D, Yi Y, et al. Consumption of the Fish Oil High-Fat Diet Uncouples Obesity and Mammary Tumor Growth through Induction of Reactive Oxygen Species in Protumor Macrophages. Cancer Res 2020;80(12):2564–74 doi 10.1158/0008-5472.CAN-19-3184. [PubMed: 32213543]
22. Zhang Y, Hao J, Sun Y, Li B. Saturated Fatty Acids Induce Ceramide-associated Macrophage Cell Death. J Vis Exp 2017(128) doi 10.3791/56535.
23. Han X. Lipidomics for studying metabolism. Nat Rev Endocrinol 2016;12(11):668–79 doi 10.1038/nrendo.2016.98. [PubMed: 27469345]
24. Wang M, Han X. Multidimensional mass spectrometry-based shotgun lipidomics. Methods Mol Biol 2014;1198:203–20 doi 10.1007/978-1-4939-1258-2_13. [PubMed: 25270931]
25. Last AR, Wilson SA. Low-carbohydrate diets. Am Fam Physician 2006;73(11):1942–8. [PubMed: 16770923]
26. McLaughlin T, Ackerman SE, Shen L, Engleman E. Role of innate and adaptive immunity in obesity-associated metabolic disease. J Clin Invest 2017;127(1):5–13 doi 10.1172/JCI88876. [PubMed: 28045397]
27. Agmon E, Stockwell BR. Lipid homeostasis and regulated cell death. Curr Opin Chem Biol 2017;39:83–9 doi 10.1016/j.cbpa.2017.06.002. [PubMed: 28645028]
28. Fajardo VA, Mikhaeil JS, Leveille CF, Saint C, LeBlanc PJ. Cardiolipin content, linoleic acid composition, and tafazzin expression in response to skeletal muscle overload and unload stimuli. Sci Rep 2017;7(1):2060 doi 10.1038/s41598-017-02089-1. [PubMed: 28515468]
29. Panov AV, Dikalov SI. Cardiolipin, Perhydroxyl Radicals, and Lipid Peroxidation in Mitochondrial Dysfunctions and Aging. Oxid Med Cell Longev 2020;2020:1323028 doi 10.1155/2020/1323028. [PubMed: 32963690]
30. Ma C, Kesarwala AH, Eggert T, Medina-Echeverz J, Kleiner DE, Jin P, et al. NAFLD causes selective CD4(+) T lymphocyte loss and promotes hepatocarcinogenesis. Nature 2016;531(7593):253–7 doi 10.1038/nature16969. [PubMed: 26934227]
31. Paradies G, Paradies V, Ruggiero FM, Petrosillo G. Role of Cardiolipin in Mitochondrial Function and Dynamics in Health and Disease: Molecular and Pharmacological Aspects. Cells 2019;8(7) doi 10.3390/cells8070728.
32. Chicco AJ, Sparagna GC. Role of cardiolipin alterations in mitochondrial dysfunction and disease. Am J Physiol Cell Physiol 2007;292(1):C33–44 doi 10.1152/ajpcell.00243.2006. [PubMed: 16899548]
33. Zhang Y, Sun Y, Rao E, Yan F, Li Q, Zhang Y, et al. Fatty acid-binding protein E-FABP restricts tumor growth by promoting IFN-beta responses in tumor-associated macrophages. Cancer Res 2014;74(11):2986–98 doi 10.1158/0008-5472.CAN-13-2689. [PubMed: 24713431]
34. Foscolou A, Critselis E, Panagiotakos D. Olive oil consumption and human health: A narrative review. Maturitas 2018;118:60–6 doi 10.1016/j.maturitas.2018.10.013. [PubMed: 30415757]
35. Mazzocchi A, Leone L, Agostoni C, Pali-Scholl I. The Secrets of the Mediterranean Diet. Does [Only] Olive Oil Matter? Nutrients 2019;11(12) doi 10.3390/nu11122941.
36. Zhou Y, Wang T, Zhai S, Li W, Meng Q. Linoleic acid and breast cancer risk: a meta-analysis. Public Health Nutr 2016;19(8):1457–63 doi 10.1017/S136898001500289X. [PubMed: 26434699]
37. Klein V, Chajes V, Germain E, Schulgen G, Pinault M, Malvy D, et al. Low alpha-linolenic acid content of adipose breast tissue is associated with an increased risk of breast cancer. Eur J Cancer 2000;36(3):335–40 doi 10.1016/s0959-8049(99)00254-3. [PubMed: 10708934]
38. Schonfeld P, Wojtczak L. Short- and medium-chain fatty acids in energy metabolism: the cellular perspective. J Lipid Res 2016;57(6):943–54 doi 10.1194/jlr.R067629. [PubMed: 27080715]

39. Frayn KN, Williams CM, Arner P. Are increased plasma non-esterified fatty acid concentrations a risk marker for coronary heart disease and other chronic diseases? Clin Sci (Lond) 1996;90(4):243–53 doi 10.1042/cs0900243. [PubMed: 8777830]
40. Tewari K, Nakayama Y, Suresh M. Role of direct effects of IFN-gamma on T cells in the regulation of CD8 T cell homeostasis. J Immunol 2007;179(4):2115–25 doi 10.4049/jimmunol.179.4.2115. [PubMed: 17675470]
41. Brehm MA, Daniels KA, Welsh RM. Rapid production of TNF-alpha following TCR engagement of naive CD8 T cells. J Immunol 2005;175(8):5043–9 doi 10.4049/jimmunol.175.8.5043. [PubMed: 16210607]
42. O'Sullivan D, van der Windt GJ, Huang SC, Curtis JD, Chang CH, Buck MD, et al. Memory CD8(+) T cells use cell-intrinsic lipolysis to support the metabolic programming necessary for development. Immunity 2014;41(1):75–88 doi 10.1016/j.immuni.2014.06.005. [PubMed: 25001241]
43. MacIver NJ, Michalek RD, Rathmell JC. Metabolic regulation of T lymphocytes. Annu Rev Immunol 2013;31:259–83 doi 10.1146/annurev-immunol-032712-095956. [PubMed: 23298210]
44. Wang R, Dillon CP, Shi LZ, Milasta S, Carter R, Finkelstein D, et al. The transcription factor Myc controls metabolic reprogramming upon T lymphocyte activation. Immunity 2011;35(6):871–82 doi 10.1016/j.immuni.2011.09.021. [PubMed: 22195744]
45. Gaschler MM, Stockwell BR. Lipid peroxidation in cell death. Biochem Biophys Res Commun 2017;482(3):419–25 doi 10.1016/j.bbrc.2016.10.086. [PubMed: 28212725]
46. Su LJ, Zhang JH, Gomez H, Murugan R, Hong X, Xu D, et al. Reactive Oxygen Species-Induced Lipid Peroxidation in Apoptosis, Autophagy, and Ferroptosis. Oxid Med Cell Longev 2019;2019:5080843 doi 10.1155/2019/5080843. [PubMed: 31737171]
47. Stavrovskaya IG, Bird SS, Marur VR, Sniatynski MJ, Baranov SV, Greenberg HK, et al. Dietary macronutrients modulate the fatty acyl composition of rat liver mitochondrial cardiolipins. J Lipid Res 2013;54(10):2623–35 doi 10.1194/jlr.M036285. [PubMed: 23690505]
48. Ayala A, Munoz MF, Arguelles S. Lipid peroxidation: production, metabolism, and signaling mechanisms of malondialdehyde and 4-hydroxy-2-nonenal. Oxid Med Cell Longev 2014;2014:360438 doi 10.1155/2014/360438. [PubMed: 24999379]
49. Zhong H, Yin H. Role of lipid peroxidation derived 4-hydroxynonenal (4-HNE) in cancer: focusing on mitochondria. Redox Biol 2015;4:193–9 doi 10.1016/j.redox.2014.12.011. [PubMed: 25598486]
50. Xia A, Zhang Y, Xu J, Yin T, Lu XJ. T Cell Dysfunction in Cancer Immunity and Immunotherapy. Front Immunol 2019;10:1719 doi 10.3389/fimmu.2019.01719. [PubMed: 31379886]

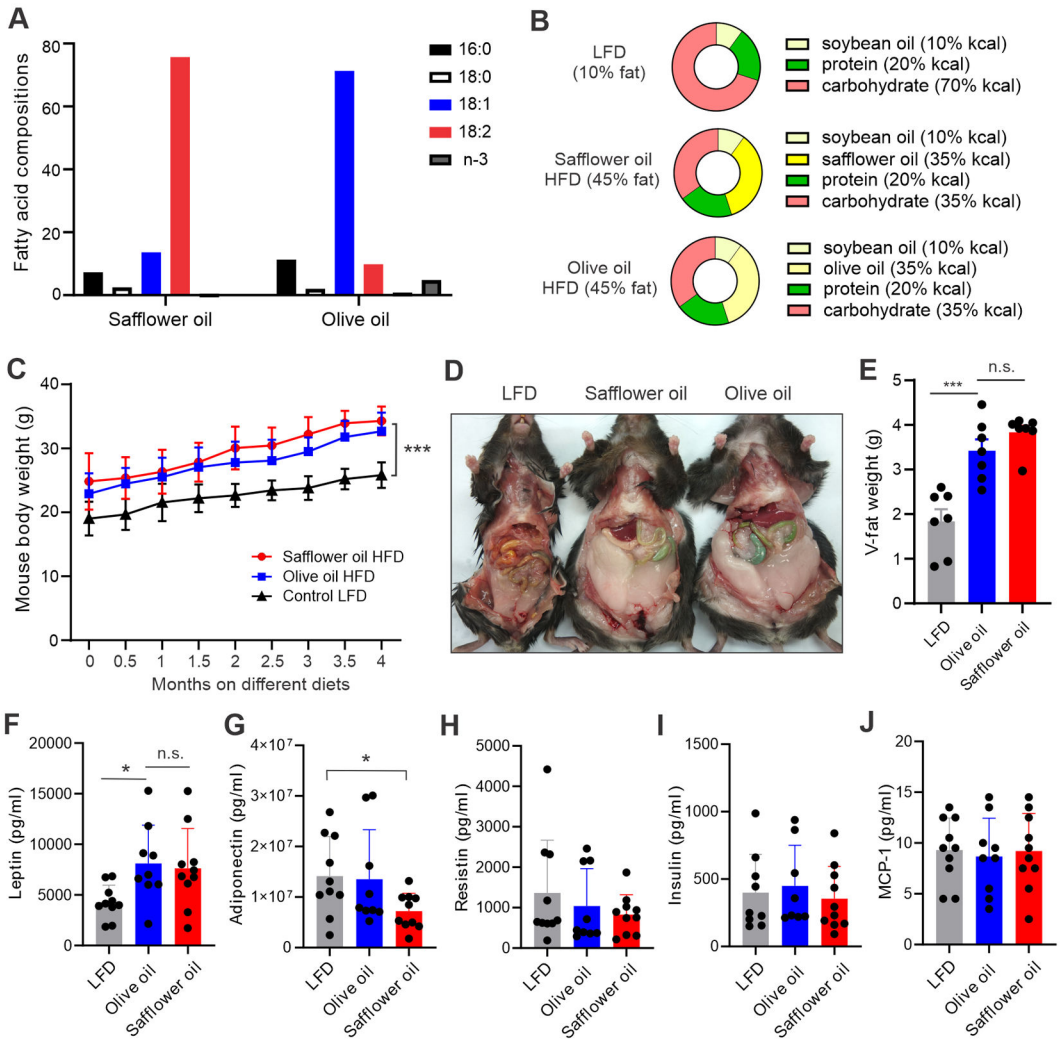

Figure 1. Safflower oil or olive oil HFD induces similar degree of murine obesity

(A) Fatty acid composition in safflower oil and olive oil.

(B) Main ingredients of custom-made safflower oil HFD, olive oil HFD and control LFD (other gradients, such as vitamins, minerals, and antioxidants, are the same).

(C) Mouse body weight on LFD (10% fat), safflower oil or olive oil HFDs (45% fat) for 4 months (n=7/group).

(D, E) Quantification of visceral fat in mice fed safflower oil, olive oil HFD or LFD obese mice for 4 months. Representative mouse images are shown in panel D. Average weight of visceral fat is shown in panel E.

(F-J) Analysis of systemic metabolic parameters, including leptin (F), adiponectin (G), resistin (H), insulin (I) and MCP-1 (J) in WT C57BL/6 mice fed with LFD, safflower oil or olive oil HFD for 4 months.

Data are shown as mean ± SEM (*p<0.05, *** p<0.001, n.s., non-significant). Also see Table S1.

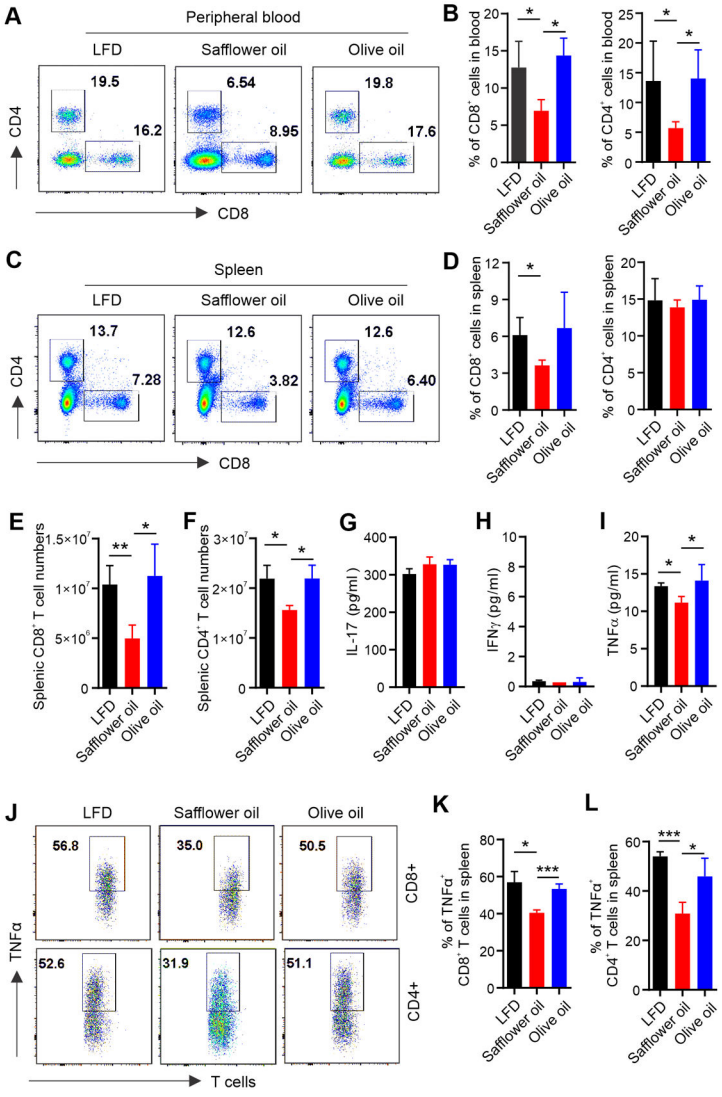

Figure 2. Safflower oil HFD-induced obese mice exhibit impaired T cell responses *in vivo*

(A, B) Flow cytometric analysis of T cell phenotype in peripheral blood of mice fed the LFD, safflower oil or olive oil HFD for 4 months. Representative flow staining of $CD8^+$ and $CD4^+$ T cells in each group is shown in panel A. Average percentages of $CD8^+$ and $CD4^+$ T cells in alive blood cells are shown in panel B.

(C, D) Flow cytometric analysis of T cell phenotype in the spleen of mice fed the LFD, safflower oil or olive oil HFD for 4 months. Representative flow staining of $CD8^+$ and $CD4^+$ T cells in each group is shown in panel C. Average percentages of $CD8^+$ and $CD4^+$ T cells in alive splenic cells are shown in panel D.

(E and F) Absolute numbers of splenic $CD8^+$ (E) and $CD4^+$ (F) T cells in mice fed the LFD, safflower oil and olive oil HFDs for 4 months.

(G-I) Analysis of the levels of IL-17A (G), IFNγ (H) and TNFα (I) production in serum from mice fed the LFD, safflower oil or olive oil HFD for 4 months by ELISA.

(J-L) Mice were fed the LFD, safflower oil or olive oil HFD for 4 months. Intracellular staining of TNFα production in splenic $CD8^+$ or $CD4^+$ T cells stimulated with PAM/

Ionomycin for 6 hours. Average percentages of TNFα production in splenic $CD8^+$ and $CD4^+$ T cells are shown in panel K and L, respectively.

Results represent 3 independent experiments. Data are shown as mean ± SEM (n=3/group, $*p < 0.05$; $**p < 0.01$; $***p < 0.001$). Also see Figure S1.

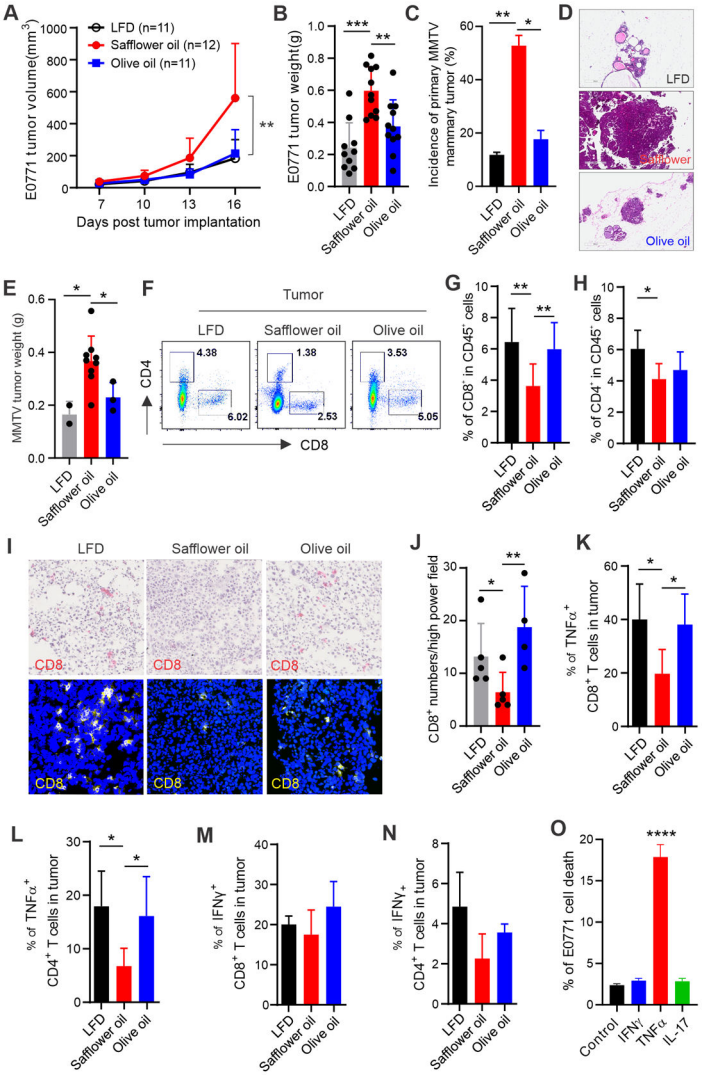

Figure 3. Safflower oil HFD-induced obesity is associated with impaired anti-tumor function of T cells

(A) Mice on the LFD, safflower or olive oil HFD for 4 months were orthotopically injected with E0771 mammary tumor cells (0.5×10^6). Tumor growth was monitored by measuring tumor size every 3 days for 16 days.

(B) E0771 tumor weight on 16 days post tumor injection in mice fed the LFD, safflower or olive oil HFD, respectively.

(C-E) Incidence of primary mammary tumors in two batches of MMTV-TGFα mice fed the LFD (n=17), safflower (n=17) or olive oil (n=18) HFD for 16 months. Representative H&E staining images of mammary tissues in each group of MMTV-TGFα mice are shown in panel D. Average tumor weight in each group is shown in panel E.

(F-H) Analysis of E0771 tumor infiltrating T cells in mice fed the LFD, safflower or olive oil HFD by flow cytometry. Average percentages of $CD8^+$ and $CD4^+$ T cells in alive $CD45^+$ cells in the tumor stroma are shown in panel G and H, respectively.

(I, J) Analysis of $CD8^+$ T cell infiltration in frozen E0771 tumor sections from mice fed the indicated diets by immunohistochemistry (red) and confocal (yellow) staining. Average numbers of $CD8^+$ T cells per high power field of confocal microscopy are shown in panel J.
(K, L) Analysis of TNFα production in E0771 tumor infiltrating $CD8^+$ (K) or $CD4^+$ (L) T cells by flow intracellular staining.
(M, N) Analysis of IFNγ production in E0771 tumor infiltrating $CD8^+$ (M) or $CD4^+$ (N) T cells by flow intracellular staining.
(O) E0771 tumor cells were cultured with indicated T cell-derived cytokines for 48 hours and the percentage of the E0771 cell death were analyzed by Annexin V/7-AAD staining. Results represent 3 independent experiments.
Results represent 3 independent experiments. Data are shown as mean ± SEM (*p<0.05, **p<0.01, ****p<0.0001). Also see Figure S2.

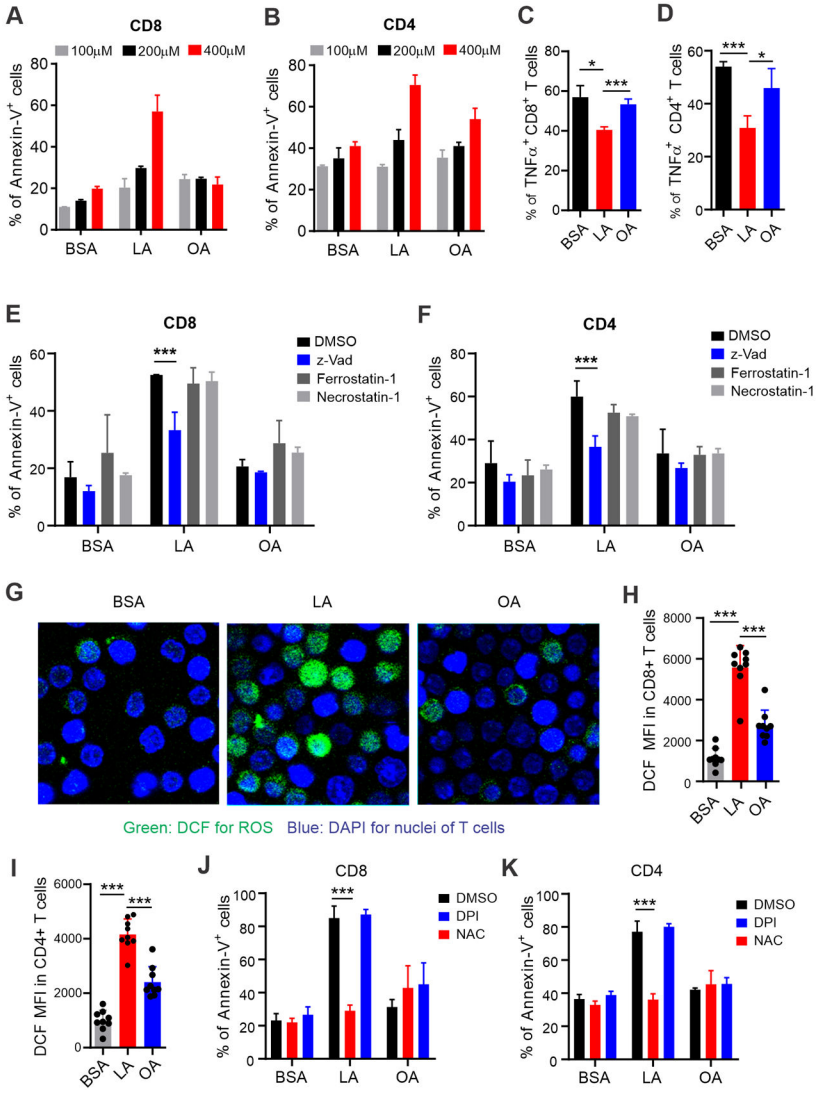

Figure 4. Analysis of apoptosis and ROS production in T cells treated with LA or OA *in vitro*.

(A, B) Splenocytes from normal wild type mice were treated with indicated concentrations of LA, OA or BSA for 20 hours. FA-induced cell death of $CD8^+$ (A) and $CD4^+$ (B) T cells were analyzed by flow cytometric annexin V staining.

(C, D) Splenocytes were treated with 400 μM LA, OA or BSA control in the presence of plate-bound ant-CD3(1μg/ml) and anti-CD28(1μg/ml) for 24 hours, PMA/ionomycin and BFA were added at the last 6 hours. Percentages of TNF-α production in $CD8^+$(C) or $CD4^+$ (D) T cells were measured by intracellular staining.

(E, F) Analysis of cell death of $CD4^+$ or $CD8^+$ T cells treated with BSA, LA, or OA (400μM) for 20 hours in the presence or absence of z-Vad, Ferrostatin-1 or Necrostatin-1 (1μM) by flow cytometry.

(G) Confocal microscopy analysis of ROS production as shown by DCF (green) in sorted T cells (DAPI, blue for nuclei) treated with BSA, LA or OA (400μM) for 30 mins.

(H, I) Measurement of fluorescent intensity of DCF in $CD8^+$ (H) or $CD4^+$ (I) T cells treated with 400μM LA, OA or BSA for 30 mins by flow cytometry.

(J, K) Cell death analysis of $CD8^+$ (J) or $CD4^+$ (K) T cells pretreated with DPI or NAC for 15mins before addition of BSA, LA, or OA (400μM) for 20 hours by flow cytometry. Results represent 3 independent experiments. Data are shown as mean ± SEM (* $p<0.05$, *** $p<0.001$). Also see Figure S3.

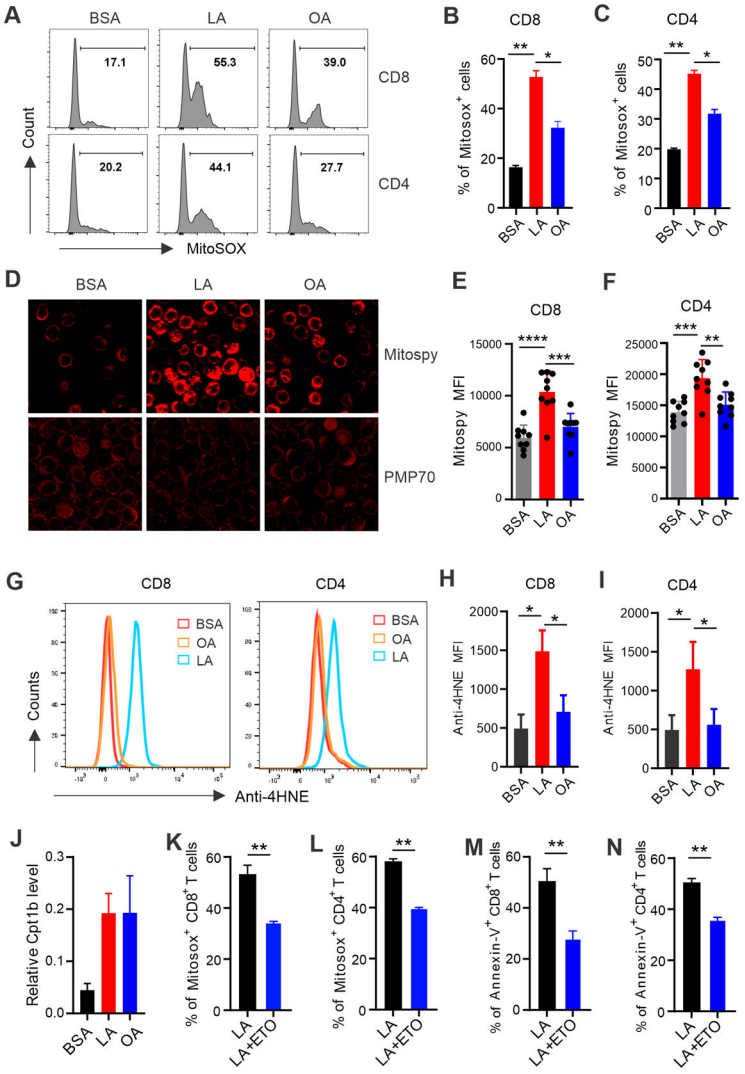

Figure 5. LA induces T cell death through promoting mitochondrial ROS production and lipid peroxidation

(A-C) Splenic T cells purified from normal C57BL/6 mice were treated with 400μM LA, OA or BSA for 20 hours. Mitochondrial ROS production in $CD8^+$ and $CD4^+$ T cells were analyzed by MitoSox staining (n=8). Average percentages of $Mitosox^+$ $CD8^+$ and $MitoSox^+$ $CD4^+$ T cells in each group are shown in panel B and C, respectively.

(D) Confocal microscopy analysis of Mitospy™ NIR DiIC1 (top) and PMP70 (70-kDA peroxisomal membrane protein) (bottom) in sorted T cells treated with BSA, LA or OA for 30 mins.

(E, F) Mitochondrial potential in $CD8^+$ (E) or $CD4^+$ (F) T cells was measured by flow cytometry with Mitospy™ NIR DiIC1 staining.

(G-I) Splenic T cells were treated with BSA, LA or OA (400μM) for 4 hours. Representative histogram of anti-4-HNE (4-hydroxynonenal) lipid peroxidation staining in $CD8^+$ or $CD4^+$ T cells was shown in panel G. Mean fluorescent intensity (MFI) of anti-4-HNE in $CD8^+$ and $CD4^+$ T cells is shown in panel H and I, respectively.

(J) Real-time PCR analysis of Cpt1b gene expression in sorted T cells treated with BSA, LA, or OA (400μM) for 12 hours.
(K, L) Analysis of mitochondrial ROS production by Mitosox staining in $CD8^+$ (K) or $CD4^+$ (L) T cells treated with LA (400μM) in the presence or absence of etomoxir (1μM), a specific Cpt1 inhibitor, for 20 hours.
(M, N) Analysis of Annexin-V^+ $CD8^+$ (M) or $CD4^+$ (N) T cells treated with LA (400μM) in the presence or absence of 1μM etomoxir for 20 hours.
Results represent 3 independent experiments. Data are shown as mean ± SEM (*p<0.05, **p<0.01, ***p<0.001, ****p<0.0001). Also see Figure S4.

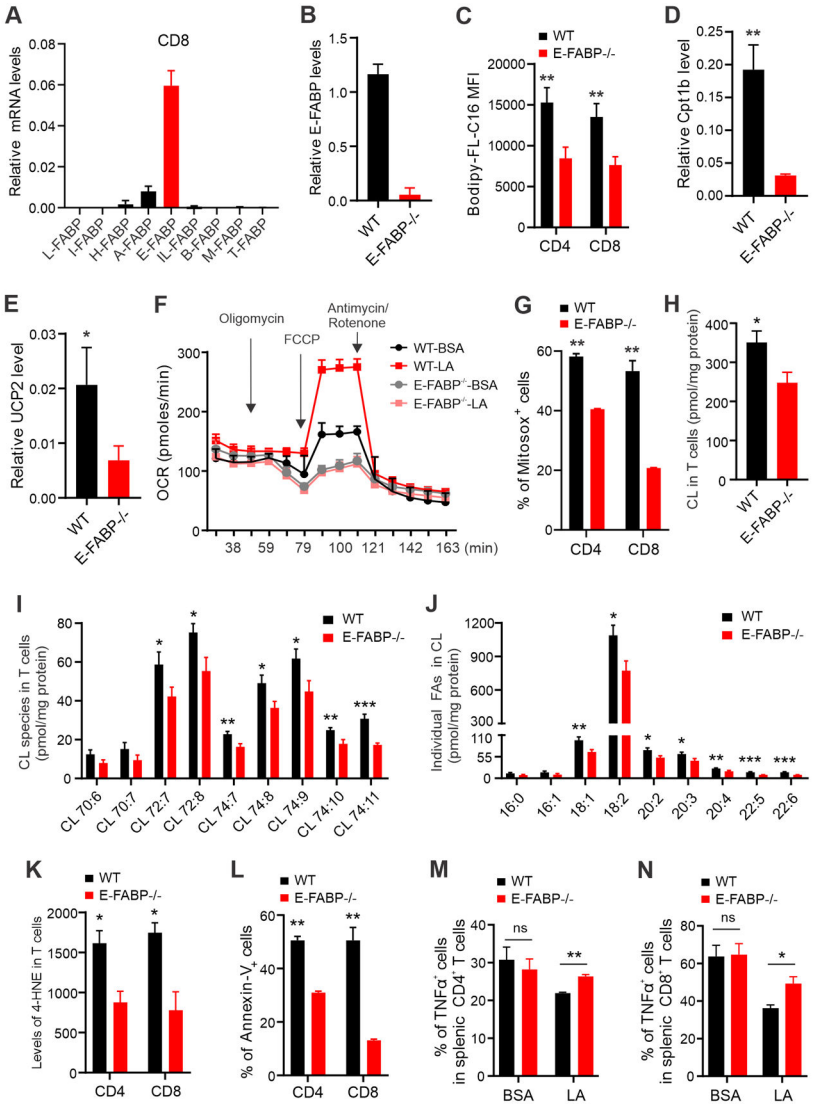

Figure 6. E-FABP expression mediates LA induced-mitochondria dysfunction in T cells

(A) Analysis of expression profile of FABP family members in purified $CD8^+$ T cells from the spleen of naïve mice by real-time PCR.

(B) Analysis of E-FABP expression in splenic $CD8^+$ T cells purified from WT and E-$FABP^{-/-}$ mice.

(C) Analysis of the uptake of Bodipy-FL-C16 fatty acid by $CD8^+$ or $CD4^+$ T cells by flow cytometric staining.

(D, E) Real-time PCR analysis of Cpt1b (D) and Ucp2 (E) expression in splenic T cells purified from WT or E-$FABP^{-/-}$ mice after treatment with LA (400μM) overnight.

(F) Splenic T cells purified from naïve WT or E-$FABP^{-/-}$ mice were seeded in ant-CD3/CD28-coated wells and treated with BSA and LA (400uM). Oxygen consumption rate (OCR) was measured in the presence of injected drugs at the indicated time points by extracellular flux analysis.

(G) Splenic T cells purified from naïve WT and E-$FABP^{-/-}$ mice were treated with LA (400μM) for 20 hours. Percentage of $Mitosox^+$ T cells was analyzed by flow cytometry.

(H-J) Splenic T cells purified from naïve WT and E-FABP$^{-/-}$ mice were treated with LA (400μM) overnight. Total (H) and individual (I) cardiolipin (CL) species and individual FAs in CLs (J) were measured by mass spectrometric analyses.

(K) Analysis of 4-HNE lipid peroxidation in LA-treated WT and E-FABP$^{-/-}$ T cells by flow cytometric staining.

(L) Analysis of LA-induced cell death in WT and E-FABP$^{-/-}$ T cells by Annexin-V staining.

(M, N) Splenic T cells purified from naïve WT or E-FABP$^{-/-}$ mice were respectively seeded in ant-CD3/CD28-coated wells and treated with BSA and LA (400uM) for 24h. PMA/ionomycin and BFA were added at the last 6 hours for analysis of intracellular production of TNFα. Representative dot plot and percentages of TNFα^{+} T cells are shown in panel M and N, respectively.

Results represent 4 independent experiments. Data are shown as mean ± SEM (n=3/group, *p<0.05, **p<0.01, ***p<0.001). Also see Figure S5.

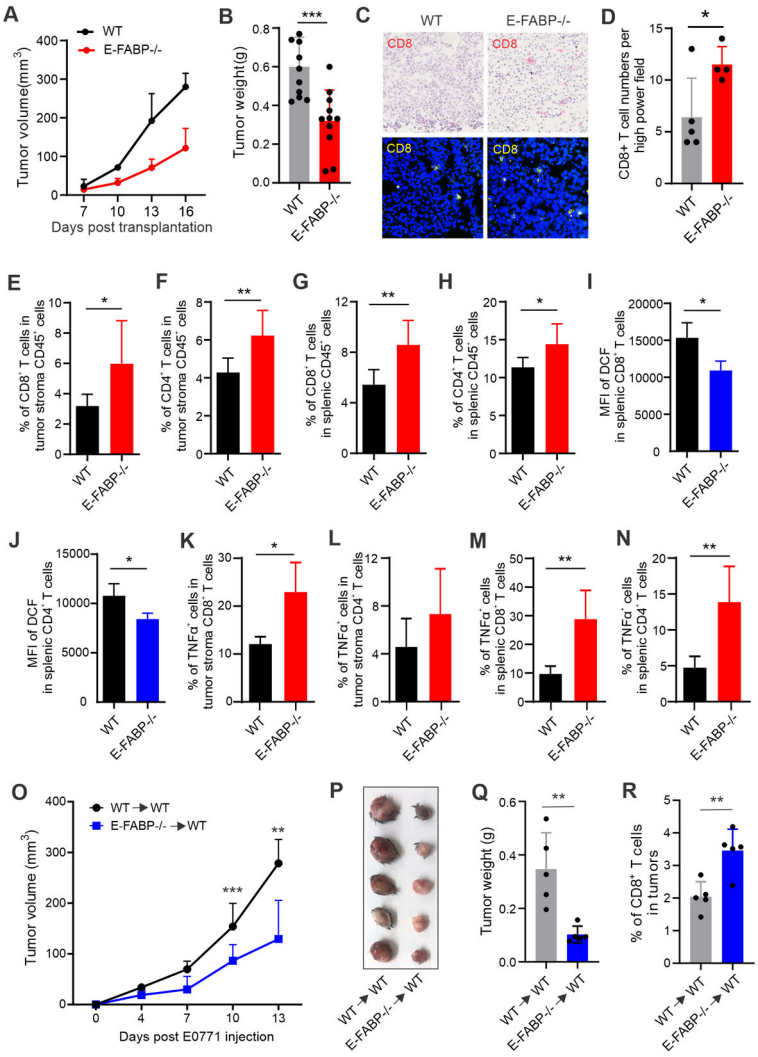

Figure 7. E-FABP deficiency mitigates safflower oil HFD-increased mammary tumor growth *in vivo*

(A, B) WT (n=11) and E-FABP$^{-/-}$ mice (n=12) fed the safflower oil HFD for 4 months were orthotopically implanted E0771 mammary tumor cells (0.5×10^6). (A) Tumor growth was monitored by measuring tumor size every 3 days for 16 days. (B) E0771 tumor weight in each group was measured 16 days post tumor injection.

(C, D) Analysis of CD8$^+$ T cell infiltration in E0771 tumor sections from WT and E-FABP$^{-/-}$ mice by immunohistochemistry (red) and confocal (yellow) staining. Average numbers of CD8$^+$ T cells per high power field of the confocal microscopy are shown in panel D.

(E, F) Analysis of the percentage of CD8$^+$ (E) and CD4$^+$ (F) T cells in alive CD45$^+$ cells in E0771 tumors of WT and E-FABP$^{-/-}$ mice.

(G, H) Analysis of the percentage of splenic CD8$^+$ (G) and CD4$^+$ (H) T cells in E0771 tumor-bearing WT and E-FABP$^{-/-}$ mice.

(I, J) Flow cytometric analysis of DCF MFI in freshly isolated splenic CD8$^+$ (I) or CD4$^+$(J) T cells from tumor-bearing WT and E-FABP$^{-/-}$ mice.

(K, L) Intracellular staining of TNFα production in tumor infiltrating $CD8^+$ (K) or $CD4^+$ (L) T cells treated with PMA/ionomycin for 6 hours.
(M, N) Intracellular staining of TNFα production in splenic $CD8^+$ (M) or $CD4^+$ (N) T cells from E0771 tumor-bearing mice after treatment with PMA/ionomycin for 6 hours.
(O-R) $CD8^+$ T cells purified from WT or E-$FABP^{-/-}$ mice fed the safflower oil HFD for 3 months were adoptively transferred into safflower oil-fed WT mice, respectively. Tumor growth was measured at the indicated time points post E0771 tumor cell implantation ($5x10^5$/mouse) (O). Tumor size and average weight are shown in panel P and Q. Tumor infiltrating $CD8^+$ T cells were analyzed by flow cytometric staining (R).
Data are shown as mean ± SEM (*p<0.05, **p<0.01, ***p<0.001). Also see Figure S6.